International Journal of Modern Physics A
Vol. 36, Nos. 11 & 12 (2021) 2140022 (13 pages)

DOI: 10.1142/S0217751X21400224

Temperature stability of the Taiji-1 satellite in operational orbit

Xiaofeng Zhang[*,†], Hong Liang[†], Heping Tan[*], Jinchao Feng[†] and Huawang Li[†,‡]

[*]*Harbin Institute of Technology, Harbin, China*

[†]*Innovation Academy for Microsatellites of the CAS, Shanghai, China*
[‡]*lihw@microsate.com*

[§]*On behalf of The Taiji Scientific Collaboration*

Received 15 September 2020
Revised 16 October 2020
Accepted 30 October 2020
Published 9 April 2021

The Taiji-1 satellite is a pioneering space technology mission designed by the Chinese Academy of Science (CAS) to test key technologies required for gravitational wave detection in space. Temperature stability is a critical element because it can couple with the gravitational wave measurement. A dedicated thermal control with a three-level control method was used on the Taiji-1 satellite science module. The simulation analysis shows that the temperature stability control level of its scientific instrument temperature stability can reach ±1.7 mK. Combined with the in-orbit temperature results, the temperature stability obtained by using the linear smoothing filter and the Kalman filter reached ±1.1 and ±0.5 mK, respectively, which were in good concerted with the simulation data, indicating that the thermal control level of Taiji-1satellite science module reached a high precision.

Keywords: Gravitational waves; Taiji Project; temperature stability; data processing.

PACS numbers: 04.80.Nn, 68.60.Dv, 44.05.+e

1. Introduction

In 1916, Einstein predicted the existence of gravitational waves, a ripple produced by the curvature of time and space.[1] Although the detection of gravitational waves is of immense research value in the study of the formation and evolution of the universe, its signal is too weak, hence it is very difficult to detect.[2]

In September 2015, the US Laser Interferometric Gravitational Wave Measurement Platform (LIGO) captured gravitational wave signals for the first time; however, due to the limitation of the length of the laser interferometric measurement arm, ground measurement equipment could only detect high-frequency gravitational wave signals. For middle and low-frequency bands with abundant gravitational wave signals, they could

All authors contributed equally to this work.
[‡]Corresponding author.
[§]For more details, please refer to article 2102002 of this Special Issue.

only be measured with an interferometric arm with a space of several million kilometers.[3,4]

After more than ten years of research and demonstration, in 2016, academicians Hu Wenrui and Wu Yueliang of the Chinese Academy of Sciences proposed the "Taiji Plan" (Taiji-1, 2 and 3). Three satellites would be deployed in the heliocentric orbit to form an interferometric arm with a length of millions of kilometers to detect gravitational wave signals in the frequency range of 0.1 mHz–1 Hz.[5] To achieve this goal, the Chinese Academy of Sciences formulated the "Taiji Plan" (Taiji-1, 2 and 3). Among them, the Taiji-1 is a near-Earth-SSO-orbiting satellite whose main task is to verify the key technology of gravitational wave detection. The high-precision and high-stability thermal control technology is a key technology in the satellite's ultra-static and ultra-stable platform.

The "Taiji-1" satellite was successfully launched in August 2019 and verified high-precision space laser interferometry technology, drag-free control technology, micro-niu-level RF Hall electric propulsion technology, and ultra-quiet and ultra-stable satellite platform control technology.[6] The high-precision temperature controller on the satellite also obtained temperature data during the experiment.

The high-precision temperature controller used by the "Taiji-1" satellite uses an analog circuit to measure temperature data on the satellite. However, the measured data includes not only temperature signals but also noise signals. Unexpectedly, in the analysis, the measured noise amplitude is larger, reaching ±5 mk, and the noise frequency is above 0.1 Hz. After analysis and processing, signal extraction is completed. At the same time, based on the satellite temperature data, the temperature simulation analysis, and temperature prediction of the core measuring instrument were carried out.

The results show that the temperature control accuracy of the "Taiji-1" satellite core measurement platform exceeds the index requirement of temperature stability $\leq$ 0.1 K/$\sqrt{\text{Hz}}$ in the 1 mHz–1 Hz frequency band by a wide margin, and achieved the mK-level temperature control accuracy. After the filtering processing, the results were consistent with the simulation design results, indicating that this filtering method is quasi-feasible and can be applied to data processing when the accuracy of the temperature collection equipment is insufficient; it also proves the multi-level temperature control method adopted by the "Taiji-1" satellite. It has reached the mK-level temperature control accuracy.

2. Taiji-1 Satellite Thermal Design

To achieve high-precision temperature control of the core measuring instrument, the "Taiji-1" satellite thermal control system must not only overcome the thermal interference of the external radiation environment but also reduce the thermal interference caused by the temperature changes of the rest of the satellites. The on-orbit test verifies that the multi-level temperature control scheme can effectively reduce these thermal interferences.

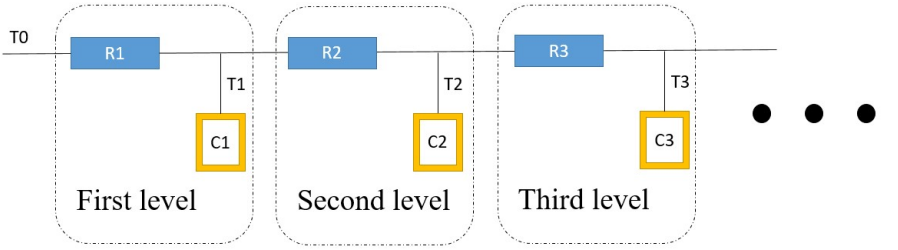

Fig. 1. Multi-level temperature control principle diagram.

2.1. *Multi-level temperature control principle*

Similar to the RC filter circuit, Fig. 1 shows the multi-stage temperature control principle. Each level of the temperature control system can be simplified into an anti-heat interference system composed of thermal resistance R and thermal capacity C, and its heat transfer differential equation is[7]

$$\frac{T_0 - T}{R} = C\frac{dT}{dt},$$

where T_0 is the ambient temperature.
T is the the temperature of the temperature control instrument,
After the Fourier transform, we can get

$$X(j\omega) = Y(j\omega) + RC\omega jY(j\omega).$$

System amplitude-frequency characteristics:

$$|H(j\omega)| = \frac{1}{\sqrt{(RC\omega)^2+1}}.$$

It can be seen from the above formula that increasing the thermal resistance R and thermal capacity C of the system can reduce the thermal interference caused by environmental temperature fluctuations. When the environmental thermal disturbance frequency decreases, the system needs to increase its thermal resistance or thermal capacity accordingly. In reality, it is not possible to increase both R and C indefinitely. At this time, the number of temperature control stages can be increased to improve the temperature control accuracy of the system. Moreover, as the number of temperature control levels increases, it improves the precise temperature control effect.

2.2. *Application of a three-level temperature control on the Taiji-1 satellite*

Figure 2 shows the "Taiji-1" satellite's adoption of a Y-direction nine-square grid layout. The core measuring instrument is located in the core cabin in the middle of the satellite, forming a relatively independent constant temperature zone. Considering the space

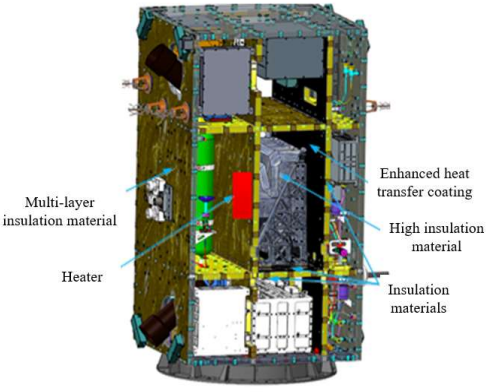

Fig. 2. The structure and layout of the "Taiji-1" satellite.

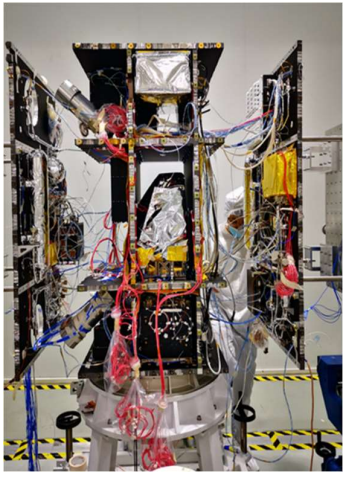

Fig. 3. The hot implementation of the "Taiji-1" satellite.

thermal environment and energy distribution of the satellite, the "Taiji-1" satellite thermal control system adopts a three-level temperature control scheme: first-level passive, second-level active and third-level passive.

(1) First-level passive temperature control

The main function of the first-level temperature control system is to increase the thermal resistance outside the core science module, maintain a relatively stable thermal environment on the outer surface of the core science assembly, and create conditions for the second-level temperature control.

In Fig. 3, from the outside to the inside, the system includes multiple layers on the outer side of the satellite, honeycomb panels on the outer side of the satellite,

conventional single planes and multiple layers on the outer side of the core science assembly. In this way, the thermal disturbance outside the satellite can reach the outer surface of the core science assembly through at least two layers of multilayer and one layer of honeycomb panels. The thermal disturbance generated by the single unit in the satellite can reach the outer surface of the core science assembly after at least one honeycomb panel + one multi-layer or two multi-layers, which greatly increases the thermal resistance outside the core science assembly.

(2) Second-level active temperature control

The second-level active temperature control system controls the surface temperature between T+0.5 K by uniformly pasting active heaters on the outer surface of the core science assembly (T is slightly higher than the outer surface temperature of the core science assembly), which is three-stage passive temperature control, creating a relatively constant thermal environment.

(3) Third-level passive temperature control

The third-level temperature control system uses low thermal conductive materials and multi-layer insulation (MLI), to minimize the heat exchange between the core measuring instrument and the inner surface of the science module to achieve absolute temperature control accuracy.

3. Temperature Results and Analysis

The analog circuit in the temperature controller completes most of the high-precision temperature measurement task of the "Taiji-1" satellite. Even though the analog circuit technology is very advanced and widely used, the collected signals will still contain some noise. This part of the noise mainly comes from electronic components and conduction circuits in analog circuits. To reduce the noise in the circuit, the temperature controller adopts micro-signal anti-interference technology, separates the digital and analog circuits into separate layouts, and uses large-area copper shielding and processing methods such as analog signal differential pair routing. However, it is increasingly difficult to eliminate the inherent noise of electronic components, and its amplitude is an interference of the order of ±5 mK.

Figure 4 shows the on-orbit temperature results of the core measuring instrument, from 20:50:00 to 21:20:00 on September 30, 2019. The temperature fluctuation range of the core instrument is 15.331–15.343℃ in 1800 s, and the temperature fluctuation is mostly concentrated in the frequency band of 0.1–1 Hz. This is inconsistent with the temperature gradual change characteristic.

The thermal capacity (C) of the core instrument is 11,000 J/K, and the total thermal resistance (R) of the core science assembly is about 2.3 K/W. From these parameters and system amplitude-frequency characteristics, it can be established that when the frequency band is 0.1–1 Hz, the amplitude of the thermal disturbance transmitted to the core instrument will be attenuated to 0.04%. Even if the six directions are superimposed on each other, the filtered disturbance amplitude will not be greater than the original 0.24%.

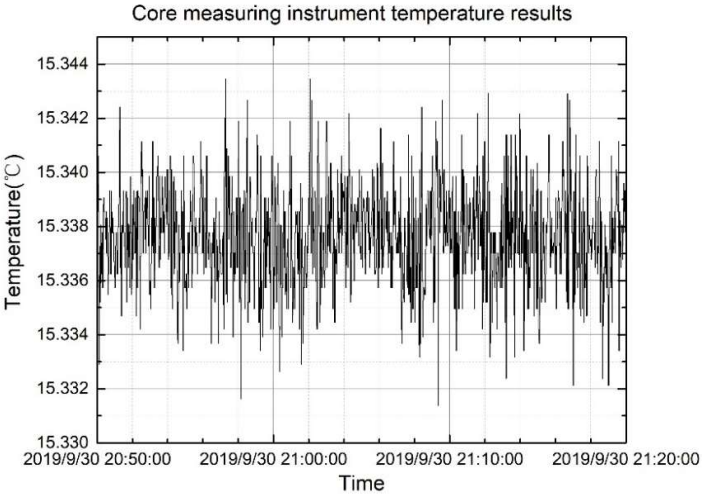

Fig. 4. Temperature curve of the core measuring instrument.

According to statistics, the maximum temperature fluctuation amplitude at the center points of the six side panels of the core science assembly during this period is 0.7 K. In 10 s, the amplitude of the temperature fluctuation of the core instrument will not exceed 1.7 mK.

To verify the correctness of the theoretical analysis, the on-orbit temperature of the six side center points of the core science assembly is used as the boundary input condition, and the core science assembly area is simulated. Figure 5 shows the calculation result. The temperature fluctuation of the core instrument within 1800 s is

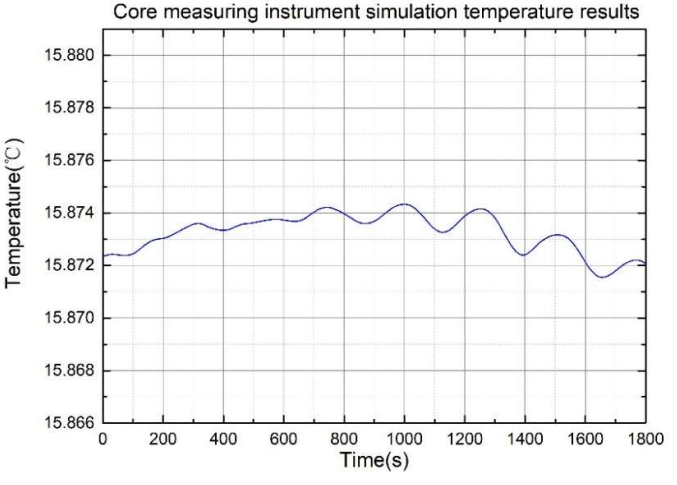

Fig. 5. Temperature curve of the core measuring instrument.

only ±1.4 mK, which is consistent with the theoretical analysis and is far lower than the on-orbit temperature measurement result, ±6 mK. It can be seen that there is a certain temperature noise in the temperature test results of the core instrument, which cannot accurately reflect the true temperature control accuracy, and further filtering is required.

4. Temperature Filtering Processing

With the development of modern digital circuits, the digital filtering technology, whose input and output are both digital signals, is widely used. It can be either an algorithm or a hardware device. According to the development law, the digital filter can be divided into a classical filter and a modern filter. The classical filter includes a window function algorithm, frequency-sampling method, and so on. The modern filter includes a free search algorithm, genetic algorithm, particle swarm optimization algorithm, etc. According to processing the signal of time domain division, can be divided into finite impulse response (FIR) and infinite impulse response (IIR) two, FIR output only depends on a finite number of input of the past and the present input, the unit impulse response sequence of IIR infinite, output depends on the past, present and future, Kodak in 1980 FIR digital filter design based on mixed integer programming techniques,[8] the free search algorithm is used for the optimization of FIR digital filter,[9] FIR digital filter is proposed based on evolutionary algorithm optimization by Mao[10] Digital filters with different structures and algorithms have different effects on the filtering effect. Therefore, the optimal design of digital filters has become a research hotspot and focus.

Bayesian filtering is a signal processing idea based on prior probability and current observation information of the system to obtain posterior probability. Its mathematical expression is as follows:

$$P(x_t \mid z_t, u_t, x_{t-1}) = \eta P(z_t \mid x_t) P(x_t \mid u_t, x_{t-1}).$$

The Kalman filtering (KF) algorithm byKalman in 1960 posited a type of linear discrete system state space equation,[13] using the system input and output data, based on known statistical characteristics of the system noise, the optimal estimation of the system state variable method is a kind of implementation for the Bayesian filtering.

With the introduction and continuous improvement of the KF theory, the KF algorithm has been widely used in aerospace systems, communication systems, radar signal processing, power systems and industrial control, and other fields, and has achieved many results. The core problem to be solved by the KF algorithm is the presence of some state quantities in the system that cannot be directly obtained by observation. Moreover, there are two methods to obtain the unknown state quantities of the system: (1) By modeling the system, using the input and output data of the system based on the system model to calculate the unknown state quantities of the system, namely $P(x_t \mid u_t, x_{t-1})$ in the above equation. This method requires a high precision of the model and the unknown disturbance will affect the precision of the solution. (2) Using the mapping relationship between the observed quantity of the system and the state quantity, estimate and solve the state quantity through the observed quantity of the

system, that is, $P(z_t \mid x_t)$ in the above equation. However, the accuracy of the mapping relationship between the observed quantity and the state quantity and the system noise will influence the solution accuracy of the system state quantity. As an important component of the modern control theory, the Kalman filter adopts the method of system state space description in expression and the form of recursion in algorithm iteration.

The temperature signal filtering methods including median filtering, limiting filtering method, the weighted recursive average filtering method, the filter, such as inertia, bang design compound digital filter algorithm, the limiter, and inertia has been proved to enhance the effect of temperature measurement of anti-interference.[12] Xiao-Wei Tang, using the median filter, the arithmetic mean filtering method, and the compound digital filter method of processing temperature data, obtained a minimum error 0.02℃ temperature measurement result.[11] The Kalman filter used to analyze the temperature signal is not widely used in aerospace. The sea surface temperature of the earth's atmosphere is an important data, but due to the attenuation caused by clouds, the common coverage rate is low. Thus, sea surface temperature using the Kalman filter to process data increases the sea surface temperature coverage from 49% to 97%.[14] The automotive industry uses the KF to handle the battery temperature simulation data, the results are compared with the experimental measurement differences within the ±0.01℃.[15]

The linear stochastic differential equation of the temperature discrete control system is as follows:

$$x_t = a_t x_{t-1} + u_t + w_t.$$

The measured value of the system is

$$z_t = c_t x_t + v_{t,}$$

where a_t,u_t and w_t are the system control parameters, control command parameters, and process noise, respectively, and c_t and v_t are system observation parameters and measurement noise, respectively. The KF system assumes that the above parameters are linear.

For the temperature measurement system of the Taiji-1 core module, the following input conditions are met:

w_t and v_t are Gaussian white noise and independent of each other, and the temperature is constant and linear $a_t = 1$, and there is no system control $u_t = 0$. The measured value directly corresponds to the output $c_t = 1$. Therefore, the linear stochastic differential equation of the temperature discrete control system is simplified as follows:

$$x_t = x_{t-1} + w_t,$$

$$z_t = x_t + v_t.$$

In addition, the covariance of the process noise and the measurement noise are R and Q, respectively, and the error variance P_t of the estimated value needs to be considered and

can be expressed as

$$P'_{t-1} = P_{t-1} + Q,$$

$$K_t = \frac{P'_{t-1}}{P'_{t-1}} + R,$$

$$P_t = (1 - K_t)P'_{t-1}.$$

where P'_{t-1} is the process error variance of the prior estimate, and K_t is Kalman Gain.

Figure 4 shows the on-orbit temperature data of the Taiji-1 core module. As can be seen from the figure, the temperature change within the observation time was 15.3376±0.006℃.

Linear smoothing filtering is a common digital filtering method. Mean filtering is carried out by assigning weights of adjacent parameters. In this paper, the temperature values are firstly filtered by five points smoothing. Considering the stability of temperature values and the same weight of sampling values at each time, the weight coefficient matrix of each point is set as:

$$b = [0.2\ 0.2\ 0.2\ 0.2\ 0.2].$$

Figure 6 shows the temperature curve after linear smooth filtering. It can be seen from the figure that the measured temperature range is 15.3348±0.003℃ and the accuracy of this group of data has been improved.

The KF method described above is used to process the data, where R=0.25 and Q=4×10^{-4}, and the filtered temperature result is shown in Fig. 7. It can be seen from the figure that the filtered temperature range is 15.3348±0.0011℃, which is more accurate and smoother than the result of linear smoothing filtering.

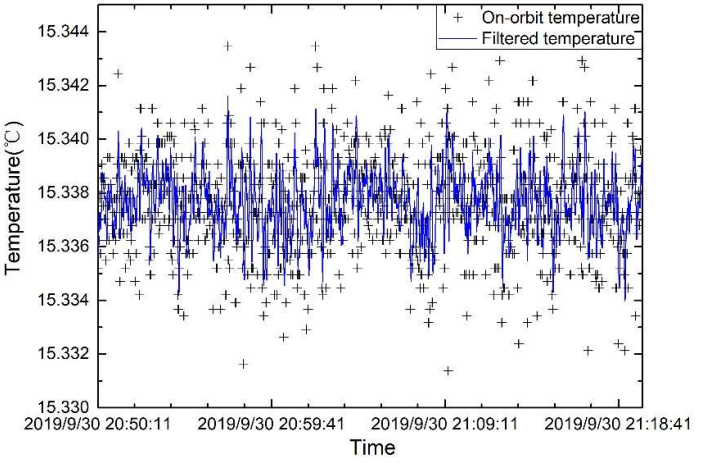

Fig. 6. Smooth filtered temperature.

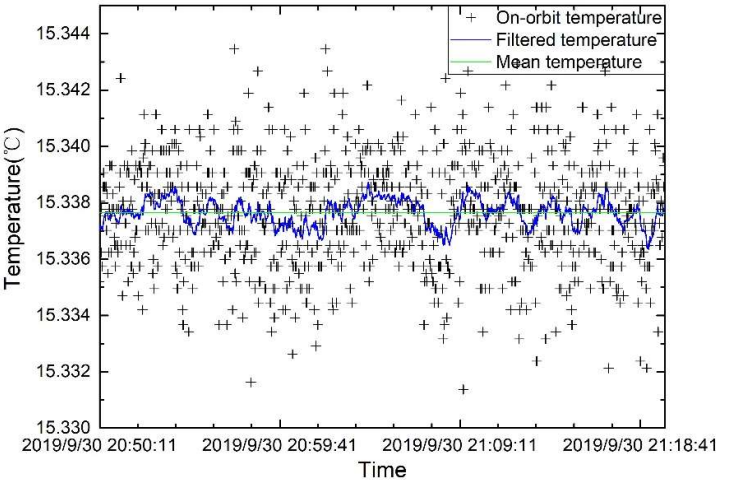

Fig. 7. Kalman filtered temperature (R=0.25, Q=4×10^{-4}).

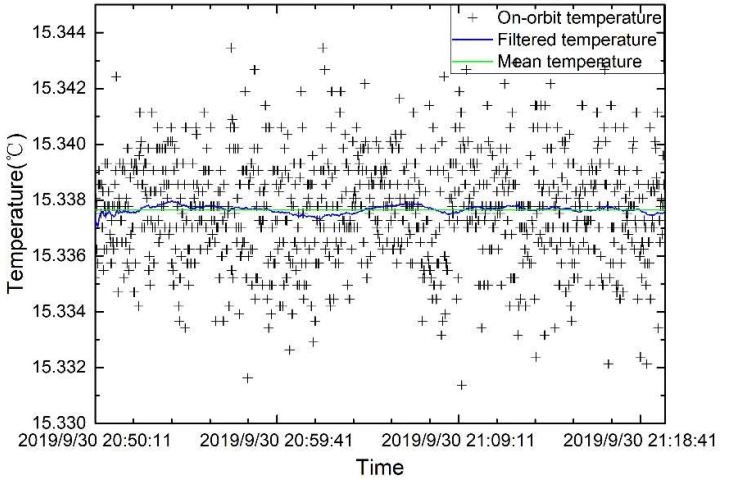

Fig. 8. Kalman filtered temperature (R=0.25, Q=4×10^{-6}).

According to the component parameters used in the satellite system, R=0.25, the error variance of the high-precision platinum resistance measurement is Q=4×10^{-6}, and the filtering results obtained are shown in Fig. 8. It can be seen from the figure that the temperature variational range is 15.3348±0.0005℃, that is, the temperature measurement accuracy of the system reaches the order of ±0.5 mK, and the curve is smoother and more continuous.

5. In-Flight Temperature Stability

Temperature stability is usually investigated with the upper and lower limits of temperature fluctuation and the variance of the measured temperature. The temperature stability of the simulation analysis and the temperature fluctuation range of in-orbit data are shown in Table 1.

It can be seen from the table that the original temperature fluctuation range in orbit is much larger than the simulation analysis value, indicating that the temperature data measured in orbit is interfered with by certain measurement noise, and the system noise needs to be removed in subsequent practical use. Both the smooth filtering and the KFcan improve the precision of measurement data, and the processed temperature data are close to the simulation analysis results, which shows that the digital filtering scheme has credibility.

The variance of the temperature data is shown in Fig. 9. The variance of the original data is 3.65×10^{-6} and the variance after smooth filtering is 1.4×10^{-6}. By adjusting the control parameters of the Kalman filter, the variance can be increased from 2.1×10^{-7} to 1.7×10^{-8}. After filtering, it is found that the stability of the temperature data is greatly improved, indicating that the actual in-orbit temperature stability of the core science assembly is good.

Table 1. Comparison of upper and lower limits of temperature fluctuation.

Simulation data	On-orbit data	Smoothing filter	Kalman filter
±1.7 mK	±6 mK	±1.1 mK	±0.5 mK

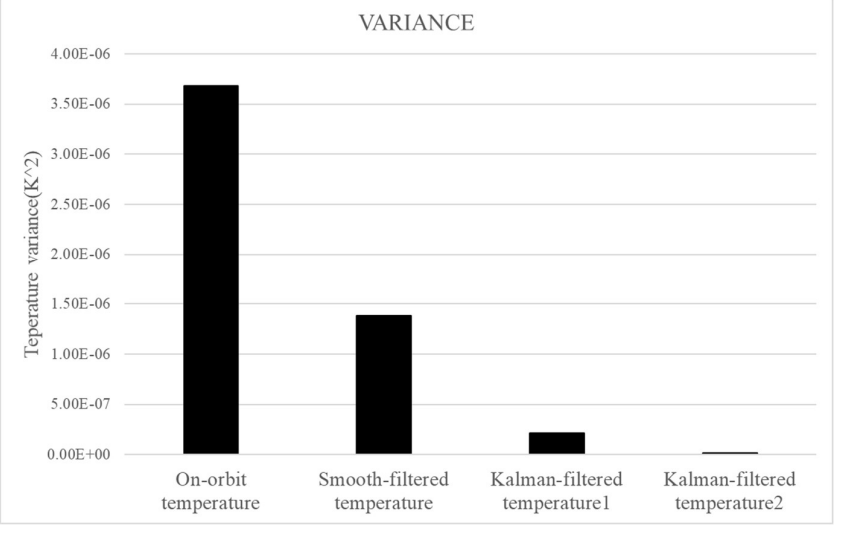

Fig. 9. The variance of data.

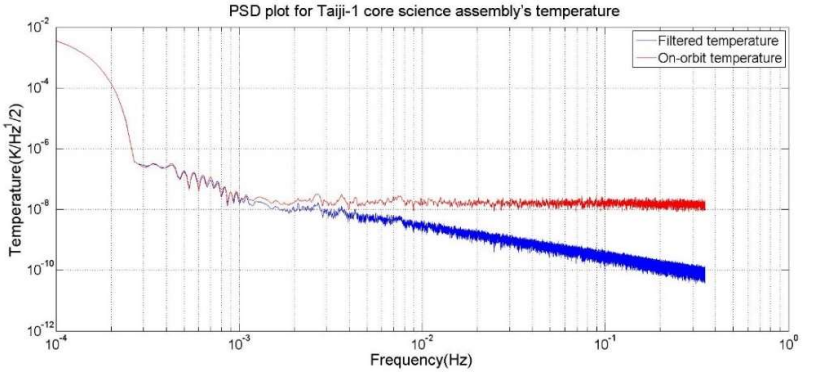

Fig. 10. PSD plot for Taiji-1 core science assembly's temperature.

The Welch algorithm was used to conduct a Power Spectral Density (PSD) analysis on the on-orbit temperature results and the temperature results after theKF; Blackman Harris window was selected to reduce wrap around leakage, and the results obtained were shown in Fig. 10. As can be seen from the diagram, at 0.1 mHz, the temperature stability of the two groups of data is 0.075 $K/Hz^{1/2}$. In the 0.1–1 mHz frequency range, the temperature of the data before and after filtering are in good consistency, which indicates that the Kalman filter will not change the frequency domain characteristics of the temperature under low-frequency stability, and because of the satellite body's low-pass filtering temperature effect, the temperature stability increases up to $10^{-6}K/Hz^{1/2}$ order of magnitude. In the frequency range from 1 mHz to 1 Hz, the effects of Quantization noise are obvious, and this noise ranges between 10^{-8}~10^{-7} $K/Hz^{1/2}$.

6. Conclusion

Based on the on-orbit temperature results of the "Taiji-1" satellite, this paper uses different filtering methods to extract the true value of the temperature data. According to the filtering principle, the high-frequency noise is eliminated, and compared with the expected simulated temperature. The results are in line with expectations, and the following conclusions are drawn:

(a) The principle of multi-level temperature control adopted by the Taiji-1 satellite is correct, and high-precision temperature control is realized. The temperature control accuracy of the core measuring instrument reaches 1.4 mk@1 mHz;

(b) The filtering method used in this article is accurate and feasible and can be used as a data processing method for the insufficient precision of temperature measuring instruments.

(c) In terms of performance, the thermal subsystem was achieved and was superior to the requirement of 10 mK. Using PSD techniques on transient temperature results for the thermal stability assessment, it can achieve the stability up to $10^{-6}K/Hz^{1/2}$. However, in the low-frequency domain below the 1 mHz, the thermal stability will increase. Some

specified method should be performed in the future to reduce the thermal noise in the low-frequency domain.

Acknowledgments

We are very glad to thank the whole Taiji-1 satellite team at Innovation Academy for Microsatellites of the CAS for all their advice and support with this thermal work. This research was supported by the Strategic Priority Program on Space Science, the Chinese Academy of Sciences, Grant No. XDA1502070702.

References

1. B. P. Abbott, R. Abbott, T. D.Abbott *et al*., *Phys. Rev. Lett.* **116**, 061102 (2016).
2. S. Weinberg, *Gravitation and Cosmology: Principles and Applications of the General Theory of Relativity*, (Wiley, New York, 1972).
3. M. Sallusti, P. Gath, D. Weise *et al*., *Class. Quantum Gravit*., **6**, 094015 (2009).
4. X. F. Gong, S. H. N. Xu, Y. F. Yuan *et al*., *Pogress Astron*. **33**,59 (2015).
5. M. Heurs, *Adv. Mech*. **43**, 415 (2013).
6. Z. R. Luo, M. Zhang, G. Jin *et al*., *J. Deep Space Exploration,* **7**, 3 (2020).
7. Z. Q. Hou and J. G. Hu, *Spacecraft Thermal Control Technology—Principle and Application* (China Science and Technology Press, Beijing, 2007), p. 273.
8. R. Mahesh and A. P. Vinod, *IEEE Trans. Computer-Aided Design Integrated Circuits Syst.* **27**, 217 (2008).
9. W. Ren, Application of the free search algorithm in digital filter optimization design, Xiangtan University (2014).
10. J. Mao, Optimization design of digital filter based on evolutionary algorithm, Henan University (2015).
11. X. Tang, *Vac. Low Temp.* **16**, 47 (2010).
12. H. Liu and X. Sun, *Electron. Meas. Technol* **4**, 21 (1999).
13. R. Kalman, *J. Basic. Eng*. **82**, 35 (1960).
14. Y. Wang, Application of Kalman filter in satellite infrared and microwave sea surface temperature data fusion, Ocean University of China (2010).
15. Y. Tian, Multi model Kalman filter SOC estimation considering battery temperature and rate characteristics, Hunan University (2018).